*antioxidants*

MDPI

*Article*

# Solvent-Dependent Redox and Polyphenol Profiles of Commercial *Andrographis paniculata*, *Silybum marianum*, and *Curcuma longa* Extracts

**Chandra Shekhar Pareek [1,2,*,†], Michał Złoch [2,*,†], Paweł Piotr Pomastowski [1,2], Justyna Walczak-Skierska [2], Joanna Rudnicka [2], Aleksandra Bogumiła Florkiewicz [2], Karolina Jakubczyk [3], Dominika Maciejewska-Markiewicz [3], Klaudia Melkis [3], Adam Lepczyński [4], Małgorzata Ożgo [4], Marta Marynowska [4], Agnieszka Herosimczyk [4], Elżbieta Redlarska [4], Mathivathana Palanisamy [1], Pratiksha Bhalerao [1], Nihal Purohit [1], Garima Kalra [1], Sharmin Sultana [1], Varunkumar Asediya [1], Brygida Ślaska [5], Paweł Grychnik [5], Athul P. Kurian [5], Katarzyna Chałaśkiewicz [6], Katarzyna Kępka-Borkowska [6], Mariusz Pierzchała [6], Prarthana Sharma [7], Avon Augustin Nalpadan [8] and Klaus Wimmers [8]**

1 Institute of Veterinary Medicine, Department of Infectious, Invasive Diseases and Veterinary Administration, Faculty of Biological and Veterinary Sciences, Nicolaus Copernicus University, ul. Szosa Bydgoska 13, 87-100 Toruń, Poland; p.pomastowski@umk.pl (P.P.P.); mathivathana@doktorant.umk.pl (M.P.); pratiksha@doktorant.umk.pl (P.B.); nihalpurohit13@doktorant.umk.pl (N.P.); garimakalra@doktorant.umk.pl (G.K.); 503646@doktorant.umk.pl (S.S.); varun@doktorant.umk.pl (V.A.)
2 Institute of Advanced Studies, Nicolaus Copernicus University, ul. Wilenska 4, 87-100 Toruń, Poland; walczak-skierska@umk.pl (J.W.-S.); jrud@umk.pl (J.R.); a.florkiewicz@umk.pl (A.B.F.)
3 Department of Human Nutrition and Metabolomics, Faculty of Health Sciences, Pomeranian Medical University in Szczecin, Broniewskiego 24, 71-460 Szczecin, Poland; karolina.jakubczyk@pum.edu.pl (K.J.); dominika.maciejewska@pum.edu.pl (D.M.-M.); klaudia.melkis@pum.edu.pl (K.M.)
4 Department of Animal Anatomy and Physiology, Faculty of Biotechnology and Animal Sciences, West Pomeranian University of Technology in Szczecin, 71-270 Szczecin, Poland; adam.lepczynski@zut.edu.pl (A.L.); malgorzata.ozgo@zut.edu.pl (M.O.); marta.marynowska@zut.edu.pl (M.M.); agnieszka.herosimczyk@zut.edu.pl (A.H.); elzbieta_lichwiarska@zut.edu.pl (E.R.)
5 Institute of Biological Bases of Animal Production, Faculty of Animal Sciences and Bioeconomy, University of Life Sciences in Lublin, 20-950 Lublin, Poland; brygida.slaska@up.lublin.pl (B.Ś.); pawel.grychnik@up.lublin.pl (P.G.); athul.kurian@up.lublin.pl (A.P.K.)
6 Department of Genomics and Biodiversity, Institute of Genetics and Animal Biotechnology of the Polish Academy of Sciences, 05-552 Jastrzębiec, Poland; k.chalaskiewicz@igbzpan.pl (K.C.); k.kepka@igbzpan.pl (K.K.-B.); m.pierzchala@igbzpan.pl (M.P.)
7 Department of Animal Biochemistry and Biotechnology, Faculty of Animal BioEngineering, University of Warmia and Mazury in Olsztyn, 10-719 Olsztyn, Poland; prarthana.sharma@doktorant.uwm.edu.pl
8 Research Institute for Farm Animal Biology (FBN), 18196 Dummerstorf, Germany; nalpadan@fbn-dummerstorf.de (A.A.N.); wimmers@fbn-dummerstorf.de (K.W.)
* Correspondence: pareekcs@umk.pl (C.S.P.); michal.zloch@umk.pl (M.Z.); Tel.: +48-56-611-26-42 (M.Z.)
† These authors contributed equally to this work.

## Abstract

Commercial botanical extracts are used as dietary antioxidants, but their activity depends on the declared marker, co-extracted phenolics, and the assay used. We characterized standardized commercial extracts of *Andrographis paniculata*, *Silybum marianum*, and *Curcuma longa* and a silymarin tablet by HPLC-ESI-MS/MS, HPLC-UV, spectrophotometric assays, and GC/MS. Markers were identified against authentic standards and quantified as 248.91 ± 6.12 mg/g andrographolide, 737.14 ± 20.31 mg/g silybin-equivalents, and 870.39 ± 6.41 mg/g curcumin; the tablet contained 66.59 ± 1.96 mg silybin-equivalents (95.13% of the declared 70 mg). Redissolution in 70% ethanol rather than boiling water increased the Folin–Ciocalteu and aluminum-complexation responses most strongly for *C. longa* and *S. marianum* (botanical × solvent interaction, $p < 0.001$), but in *C. longa*, these responses largely reflect curcuminoid solubility and assay interference rather than

Check for updates

Academic Editor: Monica Locatelli

Received: 2 October 2026
Revised: 4 November 2026
Accepted: 13 November 2026
Published: 17 November 2026

**Copyright:** © 2026 by the authors. Licensee MDPI, Basel, Switzerland. This article is an open access article distributed under the terms and conditions of the Creative Commons Attribution (CC BY) license.

polyphenol recovery. Antioxidant capacity measured by DPPH followed botanical-specific patterns that were not proportional to total phenolic response. HPLC-UV fingerprints differed between preparation media, although several retention-time assignments required mass-spectrometric confirmation. Commercial antioxidant extracts should therefore be characterized by marker-specific quantification, more than one antioxidant assay, and compositional data obtained in the same preparation medium.

**Keywords:** *Andrographis paniculata*; *Silybum marianum*; *Curcuma longa*; polyphenols; antioxidant capacity; DPPH; Folin–Ciocalteu; HPLC-MS/MS; extraction solvent

## 1. Introduction

Standardized botanical preparations occupy a dual position as chemically defined sources of bioactive constituents and as complex redox-active matrices. *Andrographis paniculata* is characterized by the diterpene lactone andrographolide and related congeners, including 14-deoxy-11,12-didehydroandrographolide [1,2]. *Silybum marianum* provides silymarin, a flavonolignan mixture containing silybin diastereomers, isosilybins, silychristin, silydianin, and taxifolin [3,4]. *Curcuma longa* is dominated by curcumin, demethoxycurcumin, and bisdemethoxycurcumin [5,6]. Because these marker families differ in polarity, ionization behavior, and radical chemistry, marker quantification and global antioxidant assays describe different aspects of the chemical composition of each preparation.

These three botanicals were selected because they are the hepatoprotective preparations used in our ongoing in vivo and in vitro studies of aflatoxin B1-induced liver dysfunction, for which the commercial materials required independent chemical characterization before use. Their declared markers (andrographolide, silymarin flavonolignans, and curcuminoids) are the primary bioactive constituents, but the commercial extracts also contain co-extracted phenolic acids and flavonoids whose contribution to antioxidant assays is rarely reported. The present study therefore characterizes both the markers and this accompanying phenolic fraction and examines how each relates to antioxidant capacity.

Redox activity within these preparations is chemically heterogeneous. Curcuminoids and flavonolignans can act as electron or hydrogen donors, stabilize phenoxyl radicals through resonance, and interfere with propagation reactions in oxidizable lipid systems [4,6]. Andrographolide does not contain a classical phenolic hydroxyl group; consequently, the direct radical-scavenging profile of an *A. paniculata* extract is expected to depend strongly on accompanying phenolic acids and flavonoids. A rigorous compositional interpretation therefore requires both a targeted marker assay and a broader phenolic fingerprint.

Extraction solvent is a primary determinant of this broader fingerprint. Water favors highly polar constituents, whereas aqueous ethanol broadens the recovered polarity range and improves access to less-polar flavonoids, flavonolignans, and curcuminoids. Modern quality control consequently combines orthogonal chromatographic data with compositional and activity-based assays rather than relying on a single declared marker [7–9].

The Folin–Ciocalteu and aluminum-complexation assays estimate reducing and flavonoid-responsive pools, respectively, whereas the DPPH, ABTS, and FRAP assays report reaction with defined radicals or oxidants under specific solvent and pH conditions [10–17]. Because each assay has a different mechanism and is subject to different interferences, more than one assay is required to characterize antioxidant capacity [18,19]. Divergence among these readouts is chemically informative: it can reveal differences in stoichiometric reactivity, solubility, reaction kinetics, and the contribution of non-phenolic reductants. GC/MS profiling of fatty-acid-derived constituents adds a further dimension because unsaturated acyl

chains are substrates for lipid peroxidation, whereas saturated species are comparatively resistant [15,20].

The objectives of this study were to: (i) identify and quantify the principal markers of commercial *A. paniculata*, *S. marianum*, and *C. longa* preparations by HPLC-ESI-MS/MS; (ii) determine how redissolution in boiling water or 70% ethanol affects total polyphenol content (TPC), total flavonoid content (TFC), individual HPLC-UV-resolved phenolics, and antioxidant capacity measured by the DPPH assay; (iii) examine the relationship between compositional and antioxidant measures; and (iv) characterize the fatty-acid-derived fraction by GC/MS.

## 2. Materials and Methods

### *2.1. Commercial Preparations*

Three commercial, standardized hydroalcoholic herbal extracts were analyzed: *A. paniculata* aerial-part extract, standardized to 20% andrographolide (Lot E02D03210-3); *S. marianum* seed extract, standardized to 80% silymarin (Lot 6D2012403-1); and *C. longa* rhizome extract, standardized to 95% curcuminoids (Lot E04D12209-3). The extracts were supplied by Swiss Herbal Institute (EUGER LTD, Blythe Road 220C London, United Kingdom). One production lot of each extract was available; the results therefore characterize these lots rather than the commercial product category as a whole. A commercial Sylimarol tablet (declared content: 70 mg silymarin per tablet; Herbapol Poznań S.A., Poznań, Poland) was analyzed in parallel. Manufacturer-supplied identity, physicochemical, heavy-metal, and microbiological specifications are reproduced in Supplementary Table S1.

### *2.2. Redissolution in Water and 70% Ethanol*

Because the commercial materials are already extracts, this step represents redissolution in two media rather than extraction of plant material; the terms aqueous preparation and 70% ethanol preparation are used throughout. For phenolic, color, and antioxidant analyses, 500 mg of each homogenized commercial material was combined with 50 mL of either boiling water or 70% (*v*/*v*) ethanol, yielding a nominal material-to-solvent ratio of 10 g/L. The preparations were shaken at 180 rpm for 15 min, sonicated for 15 min, centrifuged, and filtered through membrane filters, with protection from light throughout. The two media therefore differed in both solvent and initial temperature, and the comparison describes these two preparation procedures rather than an isolated solvent effect. For each botanical–solvent condition, three independent preparations were made and each was analyzed in triplicate, yielding nine TPC, TFC, and DPPH; color and HPLC-UV results are reported as mean ± SD determinations.

### *2.3. HPLC-MS/MS Sample Preparation and Chromatographic Conditions*

Reference standards (andrographolide; silybin; and curcumin), and commercial materials were weighed, dissolved in methanol, sonicated for 30 min, centrifuged at 12,000 rpm for 10 min, and filtered through 0.22 µm PTFE syringe filters, (Thermo Fisher Scientific, Inc., San Francisco, CA, USA) with protection from light. The tablet was crushed and processed under the same conditions. Before quantitative injection, all solutions were diluted ten-fold with mobile phase/methanol.

Analyses were performed on an LCMS-8050 triple-quadrupole mass spectrometer coupled to a Nexera HPLC system with electrospray ionization (Shimadzu, Kyoto, Japan). Separation used a Kinetex F5 column (100 × 2.1 mm, 2.6 µm; Phenomenex, Torrance, CA, USA). Mobile phase A was 0.1% aqueous formic acid and mobile phase B was acetonitrile. The gradient increased from 5% to 90% B over 0–11 min and returned to 5% B from 11–12 min. Flow rate and injection volume were 0.4 mL/min and 8 µL, respectively.

### *2.4. Qualitative Identification, MRM Acquisition, and Analytical Sensitivity*

Full-scan spectra were acquired in the positive and negative ESI modes for the extracts and for the authentic standards analyzed under identical conditions. Markers were identified by agreement of retention time, precursor ion, and MRM product ions with those of the corresponding authentic standard; congeners for which no standard was available (14-deoxy-11,12-didehydroandrographolide, demethoxycurcumin, bisdemethoxycurcumin, and taxifolin) were assigned tentatively from precursor ions and published data [5,21–23]. Quantitative acquisition used the MRM transitions and instrument potentials reported in Supplementary Table S2. Silybin-type flavonolignans were quantified with the transition $m/z$ 481.3 → 125.15 against a silybin A + B standard; because isomeric flavonolignans share this precursor and are not resolved individually by a single transition, the result is reported as silybin-equivalents and is not equivalent to the multi-component silymarin specification of the supplier. Marker contents are expressed as mg analyte per g of commercial material and converted to % $w/w$ by dividing by 10. Linearity (range, equation, and $R^2$), limits of detection and quantification, repeatability, recovery, and matrix effect were determined following ICH Q2(R2) [24] and are reported in Supplementary Table S3.

### *2.5. Total Polyphenol Content*

TPC was determined using the Folin–Ciocalteu procedure [10]. Preparations were diluted one fold before analysis. A 1.0 mL aliquot was mixed with 5.0 mL of 10% ($v/v$) Folin–Ciocalteu reagent. After 5 min, 4.0 mL of 7.5% ($w/v$) $Na_2CO_3$ was added and the mixture was incubated for 60 min at room temperature in the dark. Absorbance was measured at 765 nm on a UV-Vis spectrophotometer multiskan model (Thermo Fisher Scientific, Inc., San Francisco, CA, USA) against a reagent blank. The gallic-acid calibration (0–200 mg/L, levels) was linear. Results are reported as milligrams of gallic-acid equivalents per gram of commercial material (mg GAE/g). Because the Folin–Ciocalteu reagent also reacts with non-phenolic reductants [25], TPC is interpreted as Folin–Ciocalteu-reactive reducing capacity expressed in gallic-acid equivalents.

### *2.6. Total Flavonoid Content*

TFC was determined by aluminum complexation [11]. Preparations were diluted one fold before analysis. To 2.0 mL of sample, 0.6 mL of 5% ($w/v$) $NaNO_2$ was added. After 6 min, 0.5 mL of 10% ($w/v$) $AlCl_3$ was introduced; after a further 6 min, 3.0 mL of 4.3% ($w/v$) NaOH and 3.9 mL water were added. Absorbance was measured at 510 nm after 15 min against a sample blank in which $AlCl_3$ was replaced by water. The rutin calibration (0–120 mg/L levels) was linear. Results are reported as milligrams of rutin equivalents per gram of commercial material (mg RE/g). Curcuminoids are strongly colored and form phenolate chromophores under alkaline conditions; for *C. longa*, TFC is therefore treated as an aluminum-complexation assay response rather than as flavonoid content.

### *2.7. HPLC-UV Polyphenol Profiling*

Individual phenolics were determined with a 1260 Infinity HPLC system (Agilent Technologies, Santa Clara, CA, USA) using a Hypersil GOLD column (150 × 4.6 mm, Thermo Fisher Scientific, Waltham, MA, USA) at 25 °C and UV detection at 278 nm. Mobile phase A was 1% ($v/v$) aqueous acetic acid and mobile phase B was methanol. The gradient was: 90% A/10% B at 0–6 min; 84/16 at 7–25 min; 72/28 at 26–37 min; 65/35 at 38–47 min; 50/50 at 48–64 min; and return to 90/10 at 65–70 min. The flow rate was 0.8 mL/min and the injection volume was 30 µL. Preparations were diluted one fold before injection, and concentrations were back-calculated to the 10 g/L preparation; they are reported as mg/L of preparation and as mg/g of commercial material (mg/L ÷ 10). Compounds were assigned by

retention-time comparison with authentic standards and quantified by external calibration. Because assignments rely on retention time and one wavelength, co-elution with non-target compounds, in particular silymarin flavonolignans in *S. marianum*, cannot be excluded, and HPLC-UV results are interpreted as standard-equivalent fingerprint descriptors. The complete concentration matrix is presented in Supplementary Tables S4 and S10.

### *2.8. DPPH Radical-Scavenging Capacity*

DPPH radical-scavenging capacity was measured according to Brand-Williams et al. [12]. Preparations were diluted one fold so that the decrease in absorbance fell within the linear range of the Trolox calibration. A 0.1 mL aliquot of diluted preparation was mixed with 1.0 mL of 0.3 mM ethanolic DPPH and 2.9 mL of 96% ethanol, incubated for 30 min at room temperature in the dark, and read at 518 nm; sample color blanks (preparation with ethanol instead of DPPH) were subtracted. Results are expressed as micromoles of Trolox equivalents per gram of commercial material (µmol TE/g).

### *2.9. ABTS and FRAP Assays*

ABTS radical-cation scavenging was determined according to Re et al. [16]. Ferric reducing antioxidant power (FRAP) was determined according to Benzie and Strain [17]. Both assays were calibrated with Trolox, sample color blanks were subtracted, and results are expressed as µmol TE/g of commercial material.

### *2.10. Spectrophotometric Color Parameters*

Absorbance was recorded at 420, 520, and 620 nm. Color intensity (IC′) was calculated as $A_{420} + A_{520} + A_{620}$. Relative yellow, red, and blue contributions were calculated as $\%Y = 100 \times A_{420}/IC'$, $\%R = 100 \times A_{520}/IC'$, and $\%B = 100 \times A_{620}/IC'$. These parameters are reported as descriptive characteristics of the preparations and were not used as indicators of redox activity. The complete color dataset is reported in Supplementary Table S5 and Figure S1.

### *2.11. GC/MS Profiling of Fatty-Acid-Derived Constituents*

Approximately 50 mg of each sample was initially treated with methanol (variant M) or hexane (variant H). Two milliliters of 1% $H_2SO_4$ in methanol was added, and acid-catalyzed methanolysis was performed at 60 °C for 120 min. After cooling, 2 mL of saturated NaCl solution (6.14 M) was added. Products were extracted three times with 1 mL hexane, dried over $MgSO_4$, centrifuged at 10,000 rpm for 2 min, evaporated, and reconstituted in 100 µL methanol or hexane. Samples were coded 1H/1M (tablet), 2H/2M (silymarin extract), 3H/3M (curcumin extract), and 4H/4M (*A. paniculata* extract). No internal standard was added; so, the results are relative peak-area proportions rather than absolute fatty-acid contents.

Measurements used a 7820A gas chromatograph coupled to a 5977B mass-selective detector and an HP-5MS capillary column (30 m × 0.25 mm internal diameter, 1 µm film) (all Agilent Technologies, Santa Clara, CA, USA). Splitless injection was applied at 200 °C. The oven program was 50 °C for 2 min, 13 °C/min to 150 °C, then 5 °C/min to 230 °C with a 6 min hold. Helium flow was 1.2 mL/min. Electron ionization was 70 eV; ion-source and transfer-line temperatures were 300 and 250 °C; the scan interval was $m/z$ 35–550. Assignments were made against the NIST library using a minimum match factor of 70%. GC/MS results are expressed as normalized relative peak-area contributions. Detailed retention-time data and representative total-ion chromatograms are provided in Supplementary Table S6 and Figures S3–S10; the additional overall-profile chromatograms are shown in Figures S11–S18.

### 2.12. Data Treatment

Results are expressed as mean ± standard deviation (SD) of nine determinations (three independent preparations × three analytical replicates). For TPC, TFC, and DPPH capacity, the effects of botanical, solvent, and their interaction were tested by two-way ANOVA, and the two media were compared within each botanical by Welch's t-test with Holm correction for the three comparisons per variable (Supplementary Table S9). Because the determinations included analytical replicates of the same preparation, these tests describe differences between the preparations analyzed, not between production lots. Associations between composition and antioxidant capacity were explored across the six botanical–solvent means using Pearson and Spearman correlation; because these six means are not independent (three botanicals × two solvents), the coefficients are reported descriptively without inferential *p*-values. Relative standard deviation (RSD) was calculated as 100 × SD/mean. For GC/MS, ΣSFA was calculated as C16:0 + C18:0 and ΣUFA as C18:1 + C18:2. Analyses were performed with significance at $p < 0.05$.

## 3. Results

### 3.1. HPLC-MS/MS Identification of Principal Markers

Each commercial preparation yielded the precursor ions of its declared marker at the retention time of the corresponding authentic standard (Table 1; full-scan ESI spectra of the extracts in Supplementary Figures S19–S22). *A. paniculata* yielded andrographolide at $m/z$ 351 $[M+H]^+$ and 349 $[M-H]^-$, with $m/z$ 331 tentatively assigned to 14-deoxy-11,12-didehydroandrographolide; the $m/z$ 381 signal was not assigned. *S. marianum* and the tablet yielded $m/z$ 481 and 303 in the negative mode, assigned to silybin-type flavonolignans and, tentatively, taxifolin. *C. longa* yielded curcumin at $m/z$ 369 $[M+H]^+$ and 367 $[M-H]^-$, with demethoxycurcumin ($m/z$ 337) and bisdemethoxycurcumin ($m/z$ 307) assigned tentatively [5,21,22].

**Table 1.** Principal ions detected during qualitative HPLC-ESI-MS analysis.

| Sample | Detected Nominal Ions | Interpretation |
|---|---|---|
| *A. paniculata* extract | $m/z$ 351 $[M+H]^+$; 349 $[M-H]^-$; 381; 331 $[M-H]^-$ | Andrographolide in both polarities; ancillary ion; tentative 14-deoxy-11,12-didehydroandrographolide |
| *S. marianum* extract | $m/z$ 481 and 303 $[M-H]^-$ | Silybin-type flavonolignan marker; taxifolin |
| *C. longa* extract | $m/z$ 369 $[M+H]^+$; 367, 337, and 307 $[M-H]^-$ | Curcumin; demethoxycurcumin; bisdemethoxycurcumin |
| Commercial silymarin tablet | $m/z$ 481 and 303 $[M-H]^-$ | Silybin-type flavonolignan marker; taxifolin |

Supplementary Figures S19–S22 are full-scan spectra of the whole extracts, not product-ion spectra of isolated compounds; they document the presence of the marker ions but cannot by themselves assign every signal. Identity of the quantified markers therefore rests on the MRM transitions (andrographolide $m/z$ 349.3 → 287.25; silybin-type flavonolignans $m/z$ 481.3 → 125.15; curcumin $m/z$ 369.2 → 177.0; Supplementary Table S2) and retention times, which matched those of the authentic standards. Assignments without standards remain tentative: nominal $m/z$ 331 may also arise from water loss from deprotonated andrographolide, a single precursor mass does not distinguish silybin diastereomers from

other isomeric flavonolignans, and the successive 30 Da differences in the curcuminoid series reflect methoxy-group substitution rather than fragmentation of one precursor [5,21–23]. The tablet signal at *m*/*z* 377 remains unassigned.

### 3.2. Quantitative Marker Contents

The *S. marianum* preparation contained 737.14 ± 20.31 mg/g silybin-equivalents (73.71% *w*/*w*), *C. longa* contained 870.39 ± 6.41 mg/g curcumin (87.04% *w*/*w*), and *A. paniculata* contained 248.91 ± 6.12 mg/g andrographolide (24.89% *w*/*w*). The tablet contained 66.59 ± 1.96 mg silybin-equivalents per tablet, corresponding to 95.13% of its declared 70 mg dose. RSD values ranged from 0.74% to 2.94% (Table 2). The andrographolide content was 18–24% higher than the batch result on the supplier's certificate (20.03–21.11%). Possible contributors include differences in reference-standard purity and calibration between laboratories, residual matrix effects in external-calibration ESI-MS/MS, and the fact that the specification is a minimum (≥20%) rather than a nominal content. Silybin-equivalents and curcumin are single-analyte measures and are therefore not directly comparable with the supplier's multi-component silymarin (≥80%) and total-curcuminoid specifications.

**Table 2.** Marker contents determined by HPLC-MS/MS and descriptive comparison with manufacturer information.

| Sample | Reporting Analyte | Result | Equivalent Content/Recovery | RSD (%) | Manufacturer Information |
|---|---|---|---|---|---|
| Silymarin extract | Silybin-equivalents (*m*/*z* 481 → 125) | 737.14 ± 20.31 mg/g | 73.71% *w*/*w* | 2.76 | Generic specification: 80.1–84% silybin |
| Curcumin extract | Curcumin | 870.39 ± 6.41 mg/g | 87.04% *w*/*w* | 0.74 | Generic specification: 76.68–95.03% total curcuminoids |
| *A. paniculata* extract | Andrographolide | 248.91 ± 6.12 mg/g | 24.89% *w*/*w* | 2.46 | Generic specification: 20.03–21.11% andrographolide |
| Commercial tablet | Silybin-equivalents (*m*/*z* 481 → 125) | 66.59 ± 1.96 mg/tablet | 95.13% of label claim | 2.94 | Label: 70 mg/tablet |

### 3.3. Solvent Dependence of TPC, TFC, and DPPH Capacity

The colorimetric responses depended strongly on the botanical and the preparation medium (Table 3; Figures 1 and 2), with significant effects of botanical, solvent, and their interaction for both TPC and TFC (two-way ANOVA, all $p < 0.001$; Supplementary Table S9). In *C. longa*, the 70% ethanol preparation yielded a TPC of 101.56 ± 3.12 mg GAE/g, compared with 2.85 ± 0.02 mg GAE/g for the aqueous preparation, and a TFC of 423.06 ± 17.97 mg RE/g, compared with 3.70 ± 0.10 mg RE/g (both $p < 0.001$). A TFC 4.2 times higher than TPC is not plausible for a true flavonoid content and indicates that curcuminoids, which are not flavonoids but are strongly colored and form phenolate chromophores under the alkaline assay conditions, contributed to the absorbance at 510 nm. The approximately 36- and 114-fold increases are therefore interpreted as increases in assay response that largely reflect the much higher solubility of curcuminoids in 70% ethanol, not as recovery of polyphenols or flavonoids. *S. marianum* yielded approximately 9-fold higher TPC and 10-fold higher TFC in 70% ethanol (both $p < 0.001$). *A. paniculata* changed only modestly, from 3.08 ± 0.05 to 3.58 ± 0.05 mg GAE/g and from 4.37 ± 0.03 to 5.95 ± 0.08 mg RE/g; these small differences were statistically significant because of the low analytical SD.

**Table 3.** Total polyphenol content, total flavonoid content, and DPPH radical-scavenging capacity of aqueous and 70% ethanol preparations. Values are mean ± SD (n = 9). Within each botanical, the two media differed significantly (Welch's t-test with Holm correction, $p < 0.001$) for all variables except DPPH in *S. marianum* ($p = 0.053$).

| Botanical | Solvent | TPC (mg GAE/g) | TFC (mg RE/g) | DPPH (µmol TE/g) |
|---|---|---|---|---|
| *Curcuma longa* | Water | 2.85 ± 0.02 | 3.70 ± 0.10 | 545 ± 6 |
| *Curcuma longa* | 70% ethanol | 101.56 ± 3.12 | 423.06 ± 17.97 | 381 ± 3 |
| *Silybum marianum* | Water | 10.58 ± 0.06 | 11.21 ± 0.22 | 542 ± 45 |
| *Silybum marianum* | 70% ethanol | 94.41 ± 12.36 | 116.06 ± 9.88 | 576 ± 1 |
| *Andrographis paniculata* | Water | 3.08 ± 0.05 | 4.37 ± 0.03 | 382 ± 5 |
| *Andrographis paniculata* | 70% ethanol | 3.58 ± 0.05 | 5.95 ± 0.08 | 524 ± 6 |

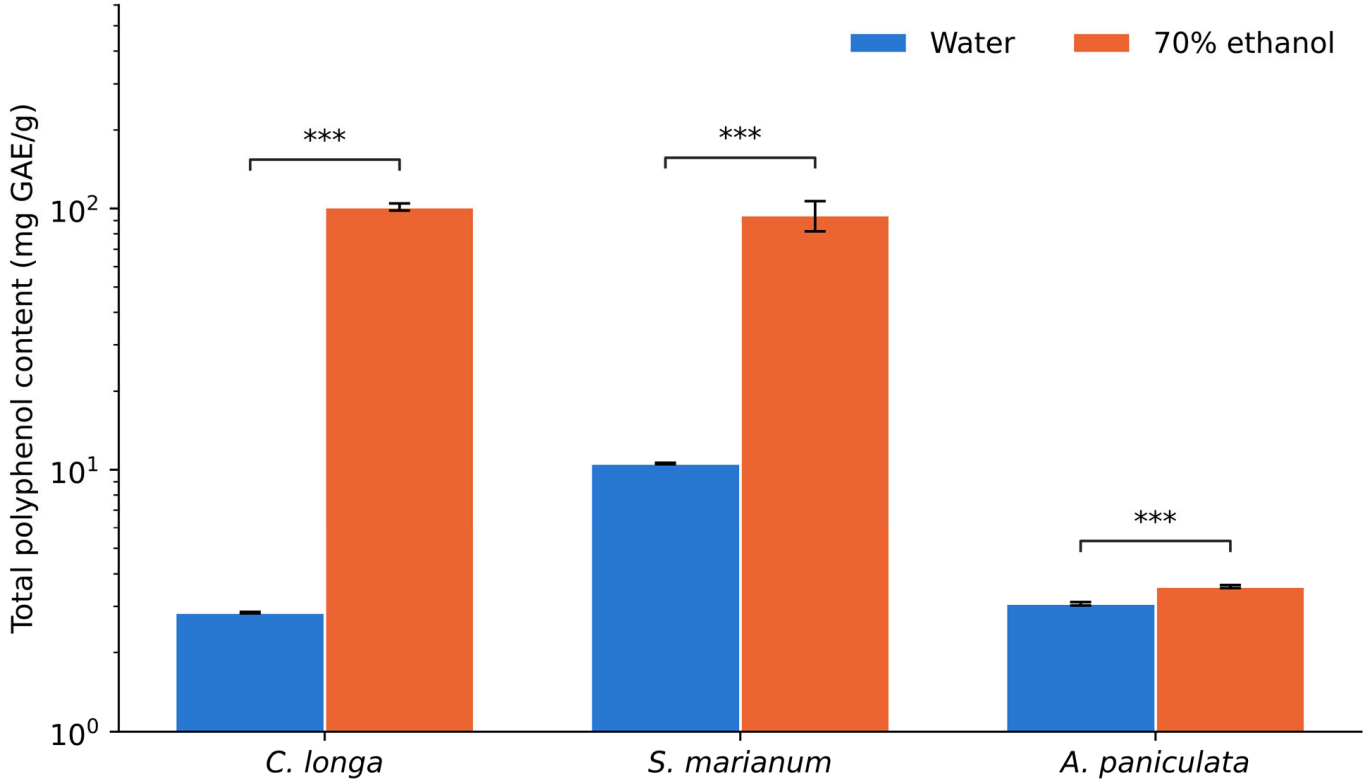



**Figure 1.** Total polyphenol content of aqueous and 70% ethanol preparations. Bars show mean ± SD (n = 9 determinations); *** $p < 0.001$ (Welch's *t*-test with Holm correction). Note the logarithmic scale.

Antioxidant capacity followed a different pattern (Table 3; Figure 3). In the DPPH assay, the *C. longa* aqueous preparation yielded 545 ± 6 µmol TE/g, compared with 381 ± 3 µmol TE/g for the ethanol preparation ($p < 0.001$), and *A. paniculata* increased from 382 ± 5 to 524 ± 6 µmol TE/g ($p < 0.001$), whereas the two *S. marianum* preparations did not differ (542 ± 45 and 576 ± 1 µmol TE/g; $p = 0.053$). For DPPH, the botanical × solvent interaction was significant ($p < 0.001$), whereas the main effect of solvent was not ($p = 0.44$). Across the six preparations, DPPH capacity varied 1.5-fold, whereas TPC varied approximately 36-fold.

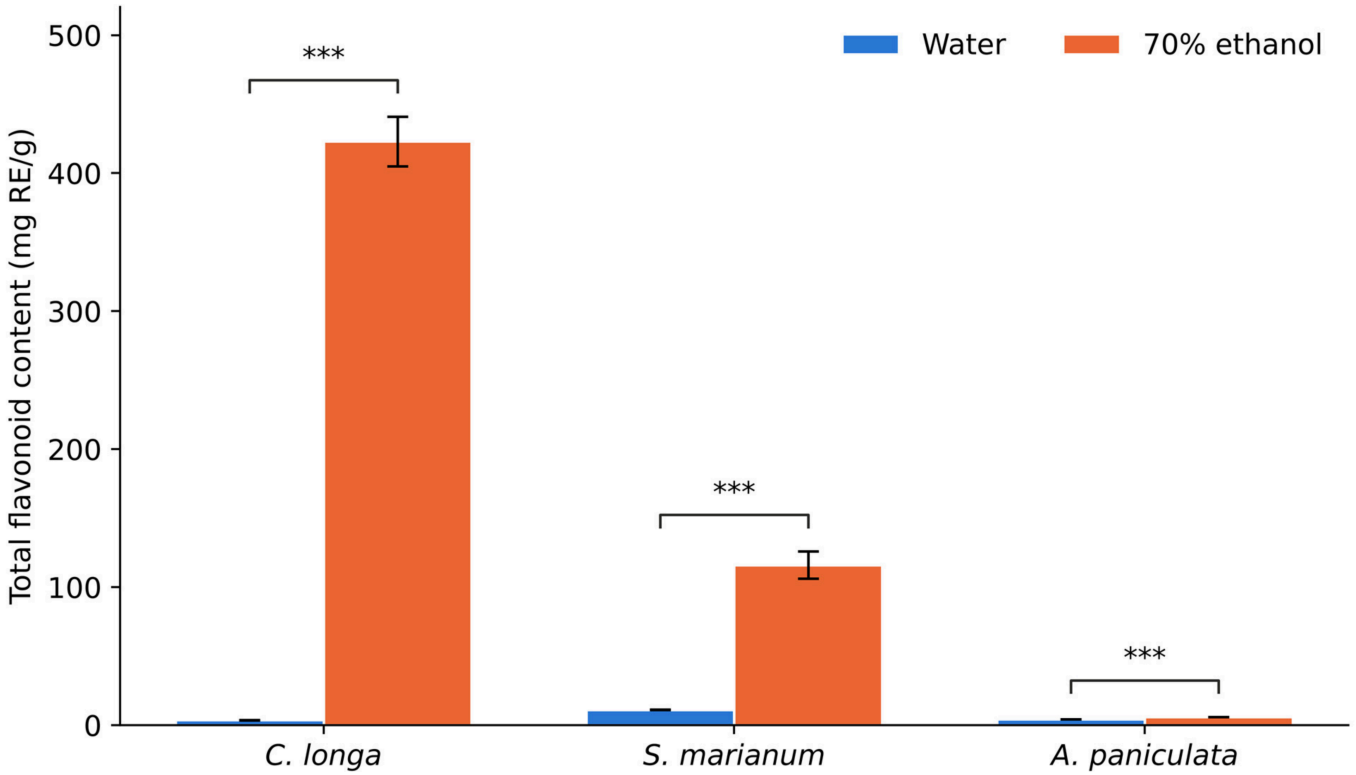



**Figure 2.** Total flavonoid content of aqueous and 70% ethanol preparations. Bars show mean ± SD (n = 9 determinations);*** $p < 0.001$ (Welch's *t*-test with Holm correction). For *C. longa*, values mainly reflect the aluminum-complexation assay response of curcuminoids.

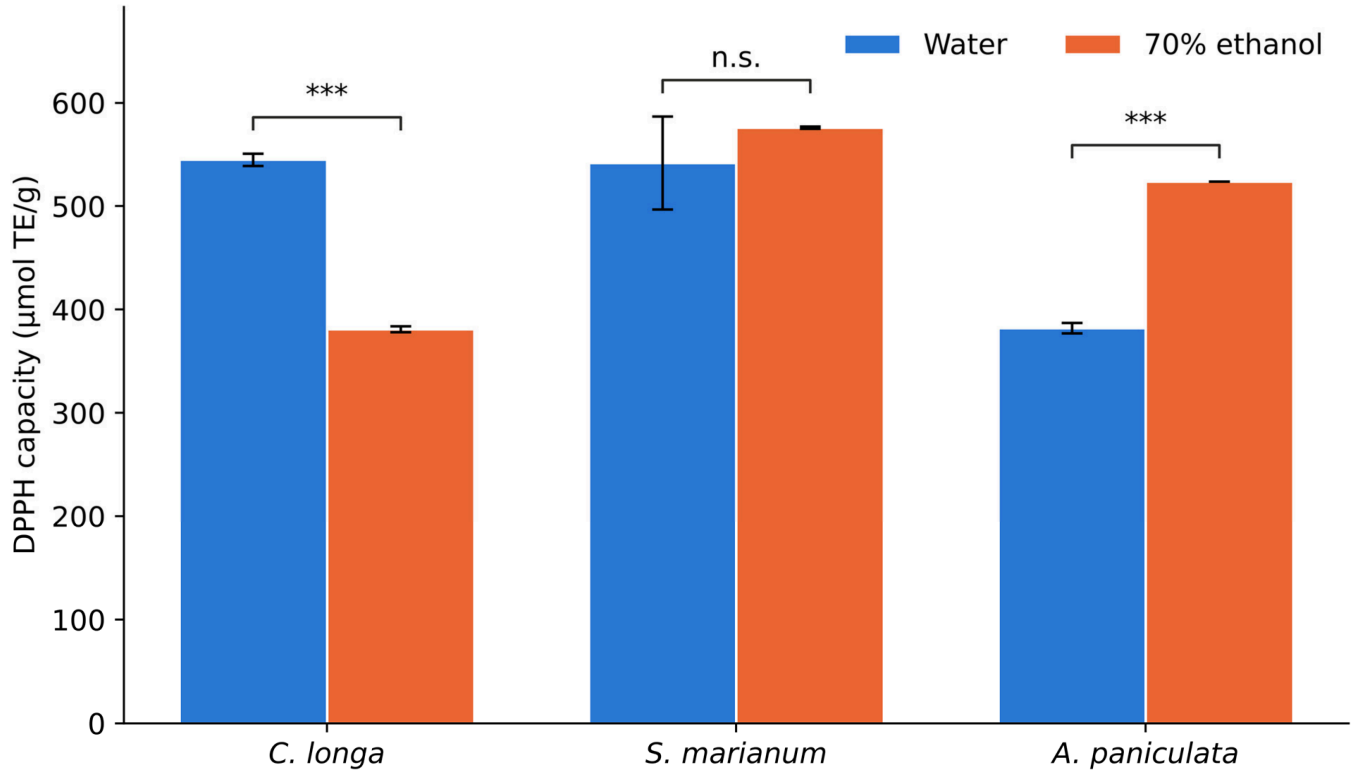



**Figure 3.** DPPH radical-scavenging capacity of aqueous and 70% ethanol preparations. Bars show mean ± SD (n = 9 determinations); *** $p < 0.001$; n.s., not significant (Welch's *t*-test with Holm correction).

### 3.4. HPLC-UV Polyphenol Fingerprints

HPLC-UV resolved botanical-specific fingerprints (Table 4) complete matrix in Supplementary Table S4; values per g of commercial material in Supplementary Table S10). In *S. marianum*, the major peak, which co-eluted with the epicatechin gallate standard, corresponded to 53.1 ± 0.8 mg/g in the aqueous and 252.7 ± 5.1 mg/g in the 70% ethanol preparation. A content of about 25% *w*/*w* for a catechin gallate is not compatible with a seed extract in which flavonolignans make up most of the mass, and together with the separately determined silybin-equivalents, it would exceed 100% *w*/*w*. This peak is therefore unlikely to be epicatechin gallate alone and probably includes co-eluting silymarin flavonolignans, which also absorb strongly near 280–290 nm. The same caution applies to the peaks assigned to myricetin and resveratrol, which were not expected in all three matrices. In *A. paniculata*, caffeic acid (15.6 and 12.4 mg/g in the aqueous and ethanol preparations) and, in ethanol only, ferulic acid (6.7 mg/g) and *p*-coumaric acid (1.0 mg/g) were the main hydroxycinnamates assigned. *C. longa* yielded low responses for the targeted panel; curcumin was quantified separately by HPLC-MS/MS.

**Table 4.** Dominant HPLC-UV-assigned phenolic peaks in aqueous and 70% ethanol preparations (retention-time assignment; mg/g of commercial material).

| Botanical | Solvent | Dominant Assigned Constituents (mg/g Commercial Material) | Quantified Analytes (n) |
|---|---|---|---|
| *C. longa* | Water | Kaempferol 2.33; apigenin 1.80; myricetin 0.83 | 6 |
| *C. longa* | 70% ethanol | Kaempferol 1.95; apigenin 1.94; sinapic acid 1.69; myricetin 1.24 | 7 |
| *S. marianum* | Water | Peak assigned to epicatechin gallate 53.1 [a]; myricetin 6.14; rutin 2.79 | 12 |
| *S. marianum* | 70% ethanol | Peak assigned to epicatechin gallate 252.7 [a]; myricetin 20.1; rutin 19.4; quercetin 8.62; resveratrol 6.24 | 7 |
| *A. paniculata* | Water | Caffeic acid 15.6; myricetin 6.95; apigenin 4.64 | 9 |
| *A. paniculata* | 70% ethanol | Myricetin 13.8; caffeic acid 12.4; ferulic acid 6.74; apigenin 6.68; *p*-coumaric acid 0.97 | 12 |

[a] Retention-time assignment; the value is not compatible with epicatechin gallate alone and probably includes co-eluting flavonolignans (see Section 3.4). Values are mg/L of the 10 g/L preparation divided by 10.

The sums of the quantified HPLC-UV entries (Supplementary Table S8) exceeded the corresponding TPC values severalfold for *S. marianum* and *A. paniculata* (for example, 32.9 mg/g versus 3.08 mg GAE/g for the aqueous *A. paniculata* preparation), whereas for *C. longa* in 70% ethanol, the sum (7.0 mg/g) was far below TPC (101.6 mg GAE/g). Because both measures refer to the same 10 g/L preparation, these discrepancies cannot be explained by units alone. They are consistent with overestimation of HPLC-UV concentrations where retention-time assignments include co-eluting compounds with high UV response and with the Folin–Ciocalteu response of curcuminoids in *C. longa* [25]. The HPLC-UV values are therefore used only to compare fingerprints between the two preparation media of the same botanical, not as absolute contents.

Within these limits, the 70% ethanol preparations differed qualitatively from the aqueous ones. In *S. marianum*, the peaks assigned to quercetin, resveratrol, rutin, and myricetin increased 23.6-, 13.5-, 6.9-, and 3.3-fold, although fewer analytes were quantified (7 versus 12). In *A. paniculata*, the number of quantified analytes increased from 9 to 12, ferulic, *p*-coumaric, and sinapic acids were detected only in ethanol, and myricetin replaced caffeic

acid as the largest peak. In *C. longa*, sinapic acid increased from 0.06 to 1.69 mg/g, whereas the flavonol and flavone peaks changed little (Supplementary Table S8).

### *3.5. Relationship Between Composition and Radical-Scavenging Capacity*

Across the six botanical–solvent means, DPPH capacity showed no positive association with TPC (Pearson r = −0.13; Spearman ρ = −0.20) or TFC (r = −0.50), whereas TPC and TFC covaried (r = 0.84). Because these coefficients are based on six non-independent means, they are descriptive only. The clearest divergence occurred in *C. longa*, in which the much higher Folin–Ciocalteu response of the ethanol preparation coincided with a 30.1% lower DPPH capacity (Figure 4).

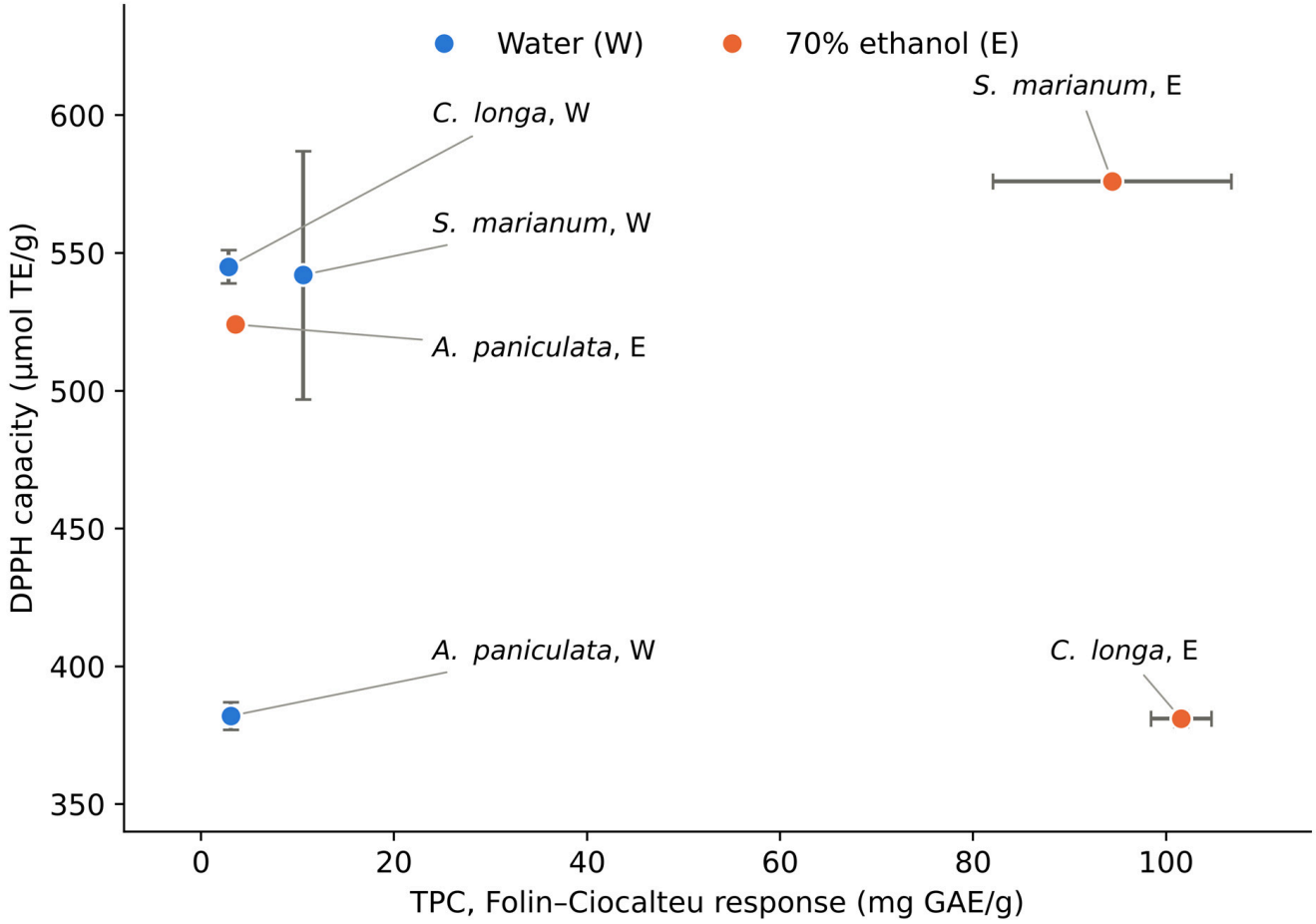



**Figure 4.** Total polyphenol content (Folin–Ciocalteu response) and DPPH radical-scavenging capacity across the six botanical–solvent means (descriptive; error bars, SD). W, water; E, 70% ethanol.

### *3.6. Color Composition*

Color composition differed between the preparations (Supplementary Table S5; Figure S1): the *C. longa* aqueous preparation was dominated by the 420 nm contribution (%Y = 87.3) and the ethanol preparation showed a higher 520 nm contribution (%R = 38.2), whereas ethanol increased the yellow contribution in *S. marianum* and *A. paniculata* (to 77.8% and 77.7%). These data are descriptive and are not interpreted in terms of redox activity.

### *3.7. GC/MS Fatty-Acid-Derived Profiles*

Palmitic- and stearic-acid-derived peaks dominated all eight preparation variants, together accounting for 83.82–100% of the identified fatty-acid-derived peak area (Table 5). The methanol-assisted *S. marianum* profile contained 3.59% C18:1 and 12.59% linoleic-acid-

derived peak area (ΣUFA = 16.18%). *A. paniculata* contained ΣUFA values of 5.14% in hexane and 8.24% in methanol. The tablet and both *C. longa* variants contained no assigned unsaturated fatty-acid-derived peaks under the applied conditions. These are relative areas normalized within the identified fatty-acid-derived peaks, obtained without an internal standard, and do not represent absolute contents; in the tablet, palmitic and stearic acid signals may originate partly from excipients such as stearate lubricants. The complete retention-time dataset and chromatograms are presented in Supplementary Table S6 and Figures S3–S10; the additional overall-profile chromatograms are shown in Figures S11–S18.

**Table 5.** Normalized relative-area composition of fatty-acid-derived peaks detected by GC/MS.

| Preparation | C16:0 (%) | C18:0 (%) | C18:1 (%) | C18:2 n-6 (%) | ΣSFA (%) | ΣUFA (%) |
|---|---|---|---|---|---|---|
| Tablet—hexane (1H) | 72.12 | 27.88 | 0.00 | 0.00 | 100.00 | 0.00 |
| Tablet—methanol (1M) | 66.67 | 33.33 | 0.00 | 0.00 | 100.00 | 0.00 |
| Silymarin extract—hexane (2H) | 71.89 | 28.11 | 0.00 | 0.00 | 100.00 | 0.00 |
| Silymarin extract—methanol (2M) | 65.38 | 18.44 | 3.59 | 12.59 | 83.82 | 16.18 |
| Curcumin extract—hexane (3H) | 71.19 | 28.81 | 0.00 | 0.00 | 100.00 | 0.00 |
| Curcumin extract—methanol (3M) | 72.79 | 27.21 | 0.00 | 0.00 | 100.00 | 0.00 |
| Andrographis extract—hexane (4H) | 69.69 | 25.17 | 2.36 | 2.78 | 94.86 | 5.14 |
| Andrographis extract—methanol (4M) | 71.61 | 20.15 | 3.72 | 4.52 | 91.76 | 8.24 |

## 4. Discussion

The analytical workflow separates three levels of information that are often conflated in botanical-product characterization: marker identity, marker content, and the composition of the accompanying matrix. The andrographolide ions in both polarities, the silybin-type $m/z$ 481 response with tentative taxifolin at $m/z$ 303, and the curcuminoid series at $m/z$ 369/367, 337, and 307 agree with established ESI-MS/MS behavior [5,21,22]. Reporting the $m/z$ 481 response as silybin-equivalents is appropriate because silymarin is a mixture and several flavonolignans share nominal precursor mass and product ions [3,22].

Quantitative agreement with commercial declarations was the closest for the tablet, which contained 95.13% of its label claim. For the extracts, measured contents must be interpreted against analyte definitions: 87.04% curcumin is not a total-curcuminoid sum, a silybin-type transition is not a multi-component silymarin assay, and the andrographolide value above the supplier's batch result points to between-laboratory differences in calibration and matrix response [22,26]. The low RSD values indicate good repeatability within the workflow; recovery and matrix-effect data are presented in Supplementary Table S3.

The distinction between marker identity and accompanying composition is important for interpreting the antioxidant data. The primary markers contribute to antioxidant capacity to different extents: curcumin and silymarin flavonolignans are established radical scavengers [4,6], whereas andrographolide, a non-phenolic diterpene lactone, is a weak direct scavenger; so, the co-extracted caffeic acid and flavonoids are expected to be particularly influential in *A. paniculata*. For *S. marianum*, purified-component experiments identified taxifolin as a stronger DPPH scavenger than the other silymarin constituents tested [4]. This comparison does not quantify its contribution in this paper, but it shows why the content of the principal silybin-type marker cannot alone describe the activity of the entire preparation. Because the markers were quantified in a separate methanolic preparation, their contribution to the antioxidant capacity of the aqueous and 70% ethanol preparations cannot be apportioned from the present data.

Independent chemical-standardization work by Muchiri and van Breemen demonstrated that individual milk-thistle constituents can respond differently to electrospray matrix effects when external calibration is compared with standard addition [23]. That finding supports retaining the response-equivalent reporting basis used in this paper, rather than interpreting one MRM transition as a complete silymarin mass balance. The present spectra and marker assay identify a targeted chemical component of each product; the solvent-resolved HPLC-UV profile describes a different, complementary component. Combining these datasets is informative precisely because neither substitutes for the other.

The strongest compositional effect was the interaction between preparation medium and botanical matrix. As expected for curcuminoids and flavonolignans, which are poorly soluble in water, 70% ethanol yielded much higher colorimetric responses for *C. longa* and *S. marianum* [6–9]; in *C. longa*, this mainly reflects curcuminoid solubility and assay response rather than recovery of additional polyphenols (Section 3.3). By contrast, *A. paniculata* showed only a 16% increase in TPC and a 36% increase in TFC, indicating that its Folin- and aluminum-reactive constituents were similarly accessible in both media.

The HPLC-UV fingerprints add qualitative information that the bulk assays cannot provide: in *A. paniculata*, ferulic and *p*-coumaric acids were detected only in the ethanol preparation, and in *S. marianum*, the peaks assigned to rutin, quercetin, and resveratrol increased in ethanol. Because these assignments rest on retention time and some values are implausibly high (Section 3.4), they are interpreted as differences in fingerprint between preparation media rather than as quantitative recoveries of individual compounds. The comparison also involved boiling water versus ethanol at a lower temperature, and therefore describes preparation outcomes under the stated conditions rather than an isolated effect of solvent polarity.

These comparisons have clear limits. HPLC-UV assignments were based on retention time at 278 nm, and the dominant *S. marianum* peak is unlikely to be epicatechin gallate alone. The HPLC-UV sums also exclude the separately measured flavonolignan and curcuminoid markers. Moreover, the Folin–Ciocalteu reagent reacts with several non-phenolic reductants [25], and curcuminoids contribute to both the Folin–Ciocalteu and aluminum-complexation responses. TPC is therefore best read as Folin–Ciocalteu-reactive reducing capacity, and in *C. longa*, both TPC and TFC are likely to overestimate polyphenol and flavonoid contents. The relationships between TPC, TFC, and antioxidant capacity (Section 3.5) must be interpreted with this in mind and are reported descriptively.

The absence of a positive relationship between TPC and DPPH capacity is consistent with the different chemistry of the assays. Folin–Ciocalteu chemistry responds to a broad reducing pool, whereas DPPH reflects the kinetics and stoichiometry of reaction with one radical in an alcoholic environment [10,12–15,18]. Preparations with similar TPC can therefore differ in radical-scavenging response if they contain different proportions of catechols, methoxylated hydroxycinnamates, curcuminoids, and non-phenolic reductants. Because DPPH was read at a single time point, part of the narrow range of DPPH values may also reflect slow-reacting constituents; the $IC_{50}$ values address this point. The strong TPC–TFC covariation indicates that the two colorimetric assays tracked a common responsive pool, whereas the weak composition–activity relationships show that this pool was not functionally homogeneous.

*A. paniculata* provides the clearest example of a gain in radical-scavenging capacity without a corresponding change in bulk phenolic response: ethanol increased TPC by only 0.50 mg GAE/g, yet DPPH capacity rose by 142 µmol TE/g. The ethanol preparation contained ferulic and *p*-coumaric acids that were not detected in water, and hydroxycinnamates with conjugated side chains can stabilize the radical products of hydrogen or electron donation [13–15]. *S. marianum* yielded similar DPPH values in both media despite

a large difference in TPC, consistent with highly reactive catecholic constituents, including flavonolignans and taxifolin [4], already present in the aqueous preparation. In *C. longa*, the lower DPPH value of the ethanol preparation despite much higher colorimetric responses shows that these responses do not translate linearly into DPPH reactivity under fixed assay conditions [6,12–15].

Structural features provide a plausible, although unproven, basis for this divergence. Catechol and galloyl groups, B-ring hydroxylation, the flavonoid 3-hydroxyl group, and glycosylation all influence DPPH reactivity [27,28]; so, preparations that differ in the compounds they contain can differ in activity independently of their total phenolic response. Because several HPLC-UV assignments require confirmation, the contributions of individual compounds cannot be reconstructed from the present data.

*A. paniculata* illustrates why a rise in DPPH response should not be assigned to the abundance of one phenolic acid. Caffeic acid decreased in ethanol despite a 37.2% increase in DPPH capacity, while myricetin, ferulic acid, and several other flavonoids became more prominent. Structure–activity experiments with hydroxybenzoic and hydroxycinnamic acids have shown that aromatic substitution and the conjugated side chain influence antioxidant behavior [29]. In addition, kinetic experiments with cinnamic acids in alcoholic media demonstrated that DPPH reduction can involve electron transfer from phenoxide species, making the solvent environment relevant to the observed response [30]. These precedents support a composition-sensitive interpretation of the present mixture, without establishing that ferulic acid is intrinsically more active than caffeic acid or that the constituents act synergistically.

The quantitative contrasts reinforce this distinction: a 4.34-fold increase in the *S. marianum* HPLC-UV sum accompanied only a 6.3% increase in mean DPPH capacity, while the 1.39-fold increase in the *C. longa* sum accompanied a 30.1% decrease. In *C. longa*, the independently determined curcumin content cannot be allocated to the aqueous and 70% ethanol preparations because the marker assay used a separate methanolic preparation. The lower DPPH response of the ethanol preparation therefore does not demonstrate curcumin antagonism, degradation, or lower intrinsic antioxidant potency. It shows instead that the measured fingerprint, bulk-equivalent assays, and a fixed-time radical assay cannot be reduced to a single concentration–activity relationship. The mechanistic interpretations above remain hypotheses consistent with the composition and literature, rather than demonstrated reaction pathways.

The GC/MS dataset provides a qualitative description of the fatty-acid-derived fraction. Unsaturated fatty acids are substrates for lipid peroxidation, whereas saturated C16:0 and C18:0 chains are comparatively resistant [15,20]. The commercial preparations showed low unsaturated relative areas, with a maximum ΣUFA of 16.18% in methanol-assisted *S. marianum* and 8.24% in methanol-assisted *A. paniculata*. This profile differs substantially from native milk-thistle seed oil, in which linoleic and oleic acids dominate [31,32], and is consistent with a processed hydroalcoholic extract rather than intact seed lipid.

Because the results are normalized relative areas obtained without an internal standard, they describe the composition of the derivatizable fatty-acid fraction, not its absolute amount, and do not allow conclusions about the total oxidizable lipid burden of the products. In the tablet, palmitic and stearic acid signals may derive partly from excipients. C18:1 was classified conservatively as an isomer because cis/trans identity cannot be resolved on a non-polar phase [33].

Perspectives. Polyphenol-rich botanical preparations are increasingly combined with lactic acid bacteria (LAB) in functional foods and feeds. LAB tolerate oxidative challenge through strain-specific antioxidant systems, and phenolic acids can be metabolized by LAB in strain- and structure-dependent ways [34–39]. The compositional and antioxidant data

reported in this paper could help select extracts and preparation media for such studies, but the present work contains no bacterial experiments, and any effect of these extracts on LAB viability or redox metabolism remains to be tested experimentally.

Limitations. This study has several limitations. (i) One lot of each commercial extract was analyzed; so, the results characterize these lots rather than the product category. (ii) The aqueous and ethanol preparations differed in both solvent and initial temperature. (iii) The nine determinations per condition included analytical replicates of the same preparation. The statistical tests therefore describe differences between the preparations analyzed rather than between production lots, and correlations across six means are descriptive. (iv) The Folin–Ciocalteu and aluminum-complexation assays are not specific for polyphenols and flavonoids and are affected by curcuminoids. (v) HPLC-UV assignments relied on retention time. (vi) GC/MS data are relative proportions. (vii) Markers were not quantified in the aqueous and 70% ethanol preparations themselves; so, their contribution to the antioxidant capacity of each preparation could not be apportioned. (viii) Antioxidant capacity was measured with a single assay (DPPH) at a single concentration and time point.

The three analytical layers are complementary. Marker analysis verifies botanical identity and marker content; colorimetric, antioxidant, and HPLC-UV data obtained in two preparation media describe how the accompanying matrix responds to the medium; and GC/MS describes the composition of the fatty-acid-derived fraction. Antioxidant capacity could not be predicted from marker percentage, TPC, or TFC alone, which supports characterizing commercial botanical extracts with marker-specific methods, more than one antioxidant assay, and compositional data obtained in the same preparation medium.

## 5. Conclusions

HPLC-MS/MS identified and quantified the principal markers of commercial *A. paniculata*, *S. marianum*, and *C. longa* extracts (24.89% andrographolide, 73.71% silybin-equivalents, and 87.04% curcumin) and showed that a commercial tablet contained 95.13% of its declared silymarin dose. Compared with boiling water, 70% ethanol strongly increased the Folin–Ciocalteu and aluminum-complexation responses of *C. longa* and *S. marianum* and only slightly increased those of *A. paniculata*; in *C. longa*, these increases largely reflect curcuminoid solubility and assay response. Antioxidant capacity measured by DPPH followed botanical-specific patterns that were not proportional to total phenolic response. HPLC-UV fingerprints differed between preparation media, but several assignments require confirmation by mass spectrometry. Commercial antioxidant botanical extracts should therefore be characterized by marker-specific quantification, more than one antioxidant assay, and compositional data obtained in the same preparation medium. Whether these preparations support probiotic bacteria under oxidative stress remains to be tested experimentally.

**Supplementary Materials:** The following supporting information can be downloaded at: https://www.mdpi.com/article/10.3390/antiox15111489/s1, Table S1: Manufacturer-supplied specifications; Table S2: HPLC-MS/MS MRM transitions and instrument potentials; Table S3: Calibration, sensitivity, repeatability, recovery, and matrix-effect data; Table S4: Complete HPLC-UV concentration matrix (mg/L); Table S5: Color parameters; Table S6: Detailed GC/MS retention-time and relative-area data; Table S7: Additional GC/MS overall-profile assignments; Table S8: Calculated HPLC-UV fingerprint descriptors; Table S9: Statistical analysis of TPC, TFC, and DPPH capacity (mean ± SD, n = 9 per botanical–solvent condition); Table S10: HPLC-UV-assigned phenolic peaks expressed per gram of commercial material (mg/g; mean ± SD; n = 3); Figure S1. Relative colour composition of aqueous and 70% ethanol preparations. W, water; E, 70% ethanol. Figure S2. Unsaturated fatty-acid-derived relative peak area across the eight GC/MS preparation variants. Figure S3. Representative fatty-acid-derived GC/MS total-ion chromatogram of the commercial silymarin tablet after hexane-assisted preparation (1H). Figure S4. Representative fatty-acid-derived GC/MS total-

ion chromatogram of the commercial silymarin tablet after methanol-assisted preparation (1M). Figure S5. Representative fatty-acid-derived GC/MS total-ion chromatogram of the silymarin extract after hexane-assisted preparation (2H). Figure S6. Representative fatty-acid-derived GC/MS total-ion chromatogram of the silymarin extract after methanol-assisted preparation (2M). Figure S7. Representative fatty-acid-derived GC/MS total-ion chromatogram of the curcumin extract after hexane-assisted preparation (3H). Figure S8. Representative fatty-acid-derived GC/MS total-ion chromatogram of the curcumin extract after methanol-assisted preparation (3M). Figure S9. Representative fatty-acid-derived GC/MS total-ion chromatogram of the *A. paniculata* extract after hexane-assisted preparation (4H). Figure S10. Representative fatty-acid-derived GC/MS total-ion chromatogram of the *A. paniculata* extract after methanol-assisted preparation (4M). Figure S11. Additional overall-profile chromatogram of the commercial silymarin tablet after hexane-assisted preparation (1H). Figure S12. Additional overall-profile chromatogram of the commercial silymarin tablet after methanolassisted preparation (1M). Figure S13. Additional overall-profile chromatogram of the silymarin extract after hexane-assisted preparation (2H). Figure S14. Additional overall-profile chromatogram of the silymarin extract after methanol-assisted preparation (2M). Figure S15. Additional overall-profile chromatogram of the curcumin extract after hexane-assisted preparation (3H). Figure S16. Additional overall-profile chromatogram of the curcumin extract after methanol-assisted preparation (3M). Figure S17. Additional overall-profile chromatogram of the *A. paniculata* extract after hexane-assisted preparation (4H). Figure S18. Additional overall-profile chromatogram of the *A. paniculata* extract after methanol-assisted preparation (4M). Figure S19. Representative positive-ion ESI mass spectrum of the *Andrographis paniculata* extract. Labelled signals include m/z 255.35, 301.35, and 331.10. These spectral features are shown without individual structural assignments; the displayed m/z 331.10 ion is not used to confirm the negative-ion m/z 331 $[M-H]^-$ assignment discussed in the manuscript. Figure S20. Representative negative-ion ESI mass spectrum of the *Silybum marianum* extract. The labelled signals at m/z 481.10 and 303.05 are consistent with the silybin-type flavonolignan and taxifolin assignments, respectively. Full-scan intensities do not define the relative concentrations of individual silymarin constituents. Figure S21. Representative positive-ion ESI mass spectrum of the *Curcuma longa* extract. Labelled signals at m/z 369.15 and 177.10 are compatible with the curcumin precursor and the product-ion channel used in the targeted assay. Figure S22. Representative negative-ion ESI mass spectrum of the commercial silymarin tablet (Sylimarol, declared content 70 mg). The labelled ions at m/z 481.10 and 303.10 correspond to the principal nominal marker ions also observed in the commercial *Silybum marianum* extract. The prominent m/z 377.10 signal remains structurally unassigned.

**Author Contributions:** Conceptualization, P.P.P., M.Z., C.S.P. and M.P. (Mariusz Pierzchała); methodology, P.P.P. and C.S.P.; formal analysis, P.P.P., G.K. and E.R.; investigation, P.P.P., J.W.-S., J.R., A.B.F., M.M. and A.H.; resources, C.S.P., M.P. (Mariusz Pierzchała) and P.P.P.; data curation, P.P.P.; writing—original draft preparation, C.S.P., M.P. (Mariusz Pierzchała), A.L. and P.P.P.; writing—review and editing, C.S.P., P.P.P., M.Z., A.L., B.Ś., M.P. (Mathivathana Palanisamy), M.O., A.A.N., J.W.-S., J.R., A.B.F., N.P., G.K., S.S., V.A., M.M., A.H., E.R., P.G., A.P.K., K.C., K.K.-B., P.S., K.W.; K.J., D.M.-M., K.M. and P.B. visualization, C.S.P., P.P.P. and M.P. (Mathivathana Palanisamy); supervision, C.S.P., P.P.P., M.Z., M.P. (Mariusz Pierzchała), A.L., B.Ś. and K.W.; project administration, C.S.P., P.P.P., M.P. (Mariusz Pierzchała) and K.W.; funding acquisition, C.S.P. and K.W. All authors have read and agreed to the published version of the manuscript.

**Funding:** This research was funded by the National Science Centre, Poland, under the OPUS-LAP program (UMO-2021/43/I/NZ9/02612) and by the Deutsche Forschungsgemeinschaft (DFG), project number 504983453 (WI 1754/18), "Multilevel molecular analysis of the hepatoprotective effect of medicinal-herb extracts in the prevention of liver dysfunction caused by aflatoxin B1 in pig as an animal model (in vivo), and hepatocyte cell-culture analysis in human and pig (in vitro)".

**Institutional Review Board Statement:** Not applicable.

**Informed Consent Statement:** Not applicable.

**Data Availability Statement:** The original contributions presented in this study are included in the article/Supplementary Materials. Further inquiries can be directed to the corresponding authors.

**Conflicts of Interest:** The authors declare no conflicts of interest.

## Abbreviations

The following abbreviations are used in this manuscript:

| | |
|---|---|
| ABTS | 2,2′-azino-bis(3-ethylbenzothiazoline-6-sulfonic acid) |
| ANOVA | analysis of variance |
| DPPH | 2,2-diphenyl-1-picrylhydrazyl |
| ESI | electrospray ionization |
| FRAP | ferric reducing antioxidant power |
| GAE | gallic-acid equivalents |
| GC/MS | gas chromatography–mass spectrometry |
| HPLC | high-performance liquid chromatography |
| $IC_{50}$ | concentration giving 50% inhibition |
| LAB | lactic acid bacteria |
| LOD | limit of detection |
| LOQ | limit of quantification |
| MRM | multiple reaction monitoring |
| MS/MS | tandem mass spectrometry |
| RE | rutin equivalents |
| RSD | relative standard deviation |
| SFA | saturated fatty acids |
| TE | Trolox equivalents |
| TFC | total flavonoid content |
| TPC | total polyphenol content |
| UFA | unsaturated fatty acids |
| UV | ultraviolet |

## References

1. Dai, Y.; Chen, S.R.; Chai, L.; Zhao, J.; Wang, Y.; Wang, Y. Overview of pharmacological activities of Andrographis paniculata and its major compound andrographolide. *Crit. Rev. Food Sci. Nutr.* **2019**, *59*, S17–S29. [CrossRef]
2. Jayakumar, T.; Hsieh, C.Y.; Lee, J.J.; Sheu, J.R. Experimental and clinical pharmacology of Andrographis paniculata and its major bioactive phytoconstituent andrographolide. *Evid. Based Complement. Altern. Med.* **2013**, *2013*, 846740. [CrossRef]
3. Wadhwa, K.; Pahwa, R.; Kumar, M.; Kumar, S.; Sharma, P.C.; Singh, G.; Verma, R.; Mittal, V.; Singh, I.; Kaushik, D.; et al. Mechanistic insights into the pharmacological significance of silymarin. *Molecules* **2022**, *27*, 5327. [CrossRef]
4. Anthony, K.P.; Saleh, M.A. Free radical scavenging and antioxidant activities of silymarin components. *Antioxidants* **2013**, *2*, 398–407. [CrossRef]
5. Jiang, H.; Somogyi, Á.; Jacobsen, N.E.; Timmermann, B.N.; Gang, D.R. Analysis of curcuminoids by positive and negative electrospray ionization and tandem mass spectrometry. *Rapid Commun. Mass Spectrom.* **2006**, *20*, 1001–1012. [CrossRef]
6. Masuda, T.; Maekawa, T.; Hidaka, K.; Bando, H.; Takeda, Y.; Yamaguchi, H. Chemical studies on antioxidant mechanism of curcumin: Analysis of oxidative coupling products from curcumin and linoleate. *J. Agric. Food Chem.* **2001**, *49*, 2539–2547. [CrossRef]
7. Noviana, E.; Indrayanto, G.; Rohman, A. Advances in fingerprint analysis for standardization and quality control of herbal medicines. *Front. Pharmacol.* **2022**, *13*, 853023. [CrossRef]
8. Balekundri, A.; Mannur, V. Quality control of traditional herbs and herbal products: A review. *Future J. Pharm. Sci.* **2020**, *6*, 67. [CrossRef]
9. Fernandes, J.M.; Silvestre, C.; Zucolotto, S.M.; Antih, J.; Vaillant, F.; Echallier, A.; Poucheret, P. Flavonoids as markers in herbal medicine quality control: Current trends and analytical perspective. *Separations* **2025**, *12*, 289. [CrossRef]
10. Singleton, V.L.; Rossi, J.A. Colorimetry of total phenolics with phosphomolybdic–phosphotungstic acid reagents. *Am. J. Enol. Vitic.* **1965**, *16*, 144–158. [CrossRef]
11. Pękal, A.; Pyrzynska, K. Evaluation of aluminium complexation reaction for flavonoid content assay. *Food Anal. Methods* **2014**, *7*, 1776–1782. [CrossRef]

12. Brand-Williams, W.; Cuvelier, M.E.; Berset, C. Use of a free radical method to evaluate antioxidant activity. *LWT Food Sci. Technol.* **1995**, *28*, 25–30. [CrossRef]
13. Munteanu, I.G.; Apetrei, C. Analytical methods used in determining antioxidant activity: A review. *Int. J. Mol. Sci.* **2021**, *22*, 3380. [CrossRef]
14. Gülçin, İ.; Alwasel, S.H. DPPH radical scavenging assay. *Processes* **2023**, *11*, 2248. [CrossRef]
15. Shahidi, F.; Zhong, Y. Measurement of antioxidant activity. *Antioxidants* **2020**, *9*, 709. [CrossRef]
16. Re, R.; Pellegrini, N.; Proteggente, A.; Pannala, A.; Yang, M.; Rice-Evans, C. Antioxidant activity applying an improved ABTS radical cation decolorization assay. *Free Radic. Biol. Med.* **1999**, *26*, 1231–1237. [CrossRef]
17. Benzie, I.F.F.; Strain, J.J. The ferric reducing ability of plasma (FRAP) as a measure of "antioxidant power": The FRAP assay. *Anal. Biochem.* **1996**, *239*, 70–76. [CrossRef]
18. Huang, D.; Ou, B.; Prior, R.L. The chemistry behind antioxidant capacity assays. *J. Agric. Food Chem.* **2005**, *53*, 1841–1856. [CrossRef]
19. Prior, R.L.; Wu, X.; Schaich, K. Standardized methods for the determination of antioxidant capacity and phenolics in foods and dietary supplements. *J. Agric. Food Chem.* **2005**, *53*, 4290–4302. [CrossRef]
20. Yin, H.; Xu, L.; Porter, N.A. Free radical lipid peroxidation: Mechanisms and analysis. *Chem. Rev.* **2011**, *111*, 5944–5972. [CrossRef]
21. Songvut, P.; Pholphana, N.; Suriyo, T.; Rangkadilok, N.; Panomvana, D.; Puranajoti, P.; Satayavivad, J. A validated LC-MS/MS method for clinical pharmacokinetics and presumptive phase II metabolic pathways following oral administration of Andrographis paniculata extract. *Sci. Rep.* **2023**, *13*, 2534. [CrossRef]
22. Lazzeroni, M.; Petrangolini, G.; Legarreta Iriberri, J.A.; Pascual Avellana, J.; Tost Robusté, D.; Cagnacci, S.; Macis, D.; Aristarco, V.; Bonanni, B.; Morazzoni, P.; et al. Development of an HPLC-MS/MS method for the determination of silybin in human plasma, urine and breast tissue. *Molecules* **2020**, *25*, 2918. [CrossRef]
23. Muchiri, R.N.; van Breemen, R.B. Chemical standardization of milk thistle (Silybum marianum L.) extract using UHPLC-MS/MS and the method of standard addition. *J. Am. Soc. Mass Spectrom.* **2024**, *35*, 1726–1732. [CrossRef]
24. International Council for Harmonisation of Technical Requirements for Pharmaceuticals for Human Use. *ICH Harmonised Guideline Q2(R2): Validation of Analytical Procedures*; ICH: Geneva, Switzerland, 2023.
25. Everette, J.D.; Bryant, Q.M.; Green, A.M.; Abbey, Y.A.; Wangila, G.W.; Walker, R.B. Thorough study of reactivity of various compound classes toward the Folin–Ciocalteu reagent. *J. Agric. Food Chem.* **2010**, *58*, 8139–8144. [CrossRef]
26. King, R.; Bonfiglio, R.; Fernandez-Metzler, C.; Miller-Stein, C.; Olah, T. Mechanistic investigation of ionization suppression in electrospray ionization. *J. Am. Soc. Mass Spectrom.* **2000**, *11*, 942–950. [CrossRef]
27. Nanjo, F.; Goto, K.; Seto, R.; Suzuki, M.; Sakai, M.; Hara, Y. Scavenging effects of tea catechins and their derivatives on 1,1-diphenyl-2-picrylhydrazyl radical. *Free Radic. Biol. Med.* **1996**, *21*, 895–902. [CrossRef]
28. Burda, S.; Oleszek, W. Antioxidant and antiradical activities of flavonoids. *J. Agric. Food Chem.* **2001**, *49*, 2774–2779. [CrossRef]
29. Natella, F.; Nardini, M.; Di Felice, M.; Scaccini, C. Benzoic and cinnamic acid derivatives as antioxidants: Structure–activity relation. *J. Agric. Food Chem.* **1999**, *47*, 1453–1459. [CrossRef]
30. Foti, M.C.; Daquino, C.; Geraci, C. Electron-transfer reaction of cinnamic acids and their methyl esters with the DPPH radical in alcoholic solutions. *J. Org. Chem.* **2004**, *69*, 2309–2314. [CrossRef]
31. Fathi-Achachlouei, B.; Azadmard-Damirchi, S. Milk thistle seed oil constituents from different varieties grown in Iran. *J. Am. Oil Chem. Soc.* **2009**, *86*, 643–649. [CrossRef]
32. Meddeb, W.; Rezig, L.; Abderrabba, M.; Lizard, G.; Mejri, M. Tunisian milk thistle: An investigation of the chemical composition and characterization of its cold-pressed seed oils. *Int. J. Mol. Sci.* **2017**, *18*, 2582. [CrossRef]
33. Mező, E.; Bufa, A.; Páger, C.; Poór, V.; Marosvölgyi, T.; Kilár, F.; Makszin, L. The role of ionic-liquid interaction in the separation of fatty-acid methyl ester polyunsaturated geometric isomers in GC–MS. *Separations* **2021**, *8*, 38. [CrossRef]
34. Rodríguez, H.; Curiel, J.A.; Landete, J.M.; de las Rivas, B.; López de Felipe, F.; Gómez-Cordovés, C.; Mancheño, J.M.; Muñoz, R. Food phenolics and lactic acid bacteria. *Int. J. Food Microbiol.* **2009**, *132*, 79–90. [CrossRef]
35. Lin, M.Y.; Yen, C.L. Antioxidative ability of lactic acid bacteria. *J. Agric. Food Chem.* **1999**, *47*, 1460–1466. [CrossRef]
36. Amaretti, A.; di Nunzio, M.; Pompei, A.; Raimondi, S.; Rossi, M.; Bordoni, A. Antioxidant properties of potentially probiotic bacteria: In vitro and in vivo activities. *Appl. Microbiol. Biotechnol.* **2013**, *97*, 809–817. [CrossRef]
37. Serrano, L.M.; Molenaar, D.; Wels, M.; Teusink, B.; Bron, P.A.; de Vos, W.M.; Smid, E.J. Thioredoxin reductase is a key factor in the oxidative stress response of Lactobacillus plantarum WCFS1. *Microb. Cell Factories* **2007**, *6*, 29. [CrossRef]

38. Rogozinska, M.; Korsak, D.; Mroczek, J.; Biesaga, M. Catabolism of hydroxycinnamic acids in contact with probiotic Lactobacillus. *J. Appl. Microbiol.* **2021**, *131*, 1464–1473. [CrossRef]
39. Arcanjo, N.O.; Andrade, M.J.; Padilla, P.; Rodríguez, A.; Madruga, M.S.; Estévez, M. Resveratrol protects Lactobacillus reuteri against $H_2O_2$-induced oxidative stress and stimulates antioxidant defenses through upregulation of the dhaT gene. *Free Radic. Biol. Med.* **2019**, *135*, 38–45. [CrossRef]

**Disclaimer/Publisher's Note:** The statements, opinions and data contained in all publications are solely those of the individual author(s) and contributor(s) and not of MDPI and/or the editor(s). MDPI and/or the editor(s) disclaim responsibility for any injury to people or property resulting from any ideas, methods, instructions or products referred to in the content.